#6177

METHODS FOR PREDICTING AIR CHANGE EFFICIENCY

Yuguo Li, Laszlo Fuchs, Sture Holmberg*

Department of Gasdynamics
Royal Institute of Technology
S- 100 44 Stockholm
SWEDEN

* Ventilation Division
National Institute of Occupational Health
S-171 84 Solna
SWEDEN

SUMMARY

Three methods for predicting air age and air change efficiency in ventilated rooms are developed and compared. They are: a *transient method* in which a time-dependent concentration equation is solved; a *steady-state method* in which a steady-state equation of air age is solved; and a *particle-marker method* in which particles are tracked explicitly. In the first two methods, a multigrid technique is used to solve the discrete problems. The methods are used to calculate the air change efficiency in a test room. The calculated results are compared with measured data. It is shown that the first two methods are the most efficient and reliable for predicting the local mean ages of indoor air, and the third method is the most efficient and reliable for predicting air change efficiency.

METHODS FOR PREDICTING AIR CHANGE EFFICIENCY

Yuguo Li, Laszlo Fuchs, Sture Holmberg*

Department of Gasdynamics
Royal Institute of Technology
S– 100 44 Stockholm
SWEDEN

* Ventilation Division
National Institute of Occupational Health
S–171 84 Solna
SWEDEN

INTRODUCTION

The success of a ventilation design can be assessed in terms of air change efficiency and ventilation effectiveness [1–4]. Air change efficiency is a measure of how effectively the air in a room is replaced by fresh air from the ventilation system; ventilation effectiveness is a measure of how quickly a contaminant is removed from the room. They are both important factors in ventilation design. Only the air change efficiency and the related local mean age of the air are considered in this paper, but most of the methods developed and discussed can be used to find the ventilation effectiveness. In general, two procedures are available, an experimental and a numerical. The air change efficiency can be estimated in an existing building by measuring the concentration changes from a particular pollutant source within a room. If the pollutant source is not known, the age of the air can be found by using tracer gas.

Tracer gas is used because the measurement of air flow is technically difficult and expensive. The local mean age distribution has been experimentally investigated by Sandberg [5]. A simple tracer gas method has been suggested by Roulet et al [6] to map the mean age distribution of air in a room. Davidson and Olsson [7] claim that numerical calculations give a more detailed picture of the age distribution than experiments do. The common procedures used in the experiment (step–up or step–down) can also be used in numerical methods. Davidson and Olsson [7] and Fontaine et al [8] have successfully used a step–down approach to calculate the age distribution in ventilated rooms.

The purpose here is threefold: to describe a fast numerical method for predicting air velocity; to describe a computational method to speed up the conventional approach; and to develop a new method for predicting the air change efficiency.

One major disadvantage of the conventional numerical algorithms, like the SIMPLE and MAC methods commonly used to simulate the indoor airflow, is their slow convergence rate. The finer the grid, the slower the convergence. This difficulty could be reduced by using acceleration techniques such as the multigrid method. These have not yet been widely used in indoor airflow simulation. In this article, the multigrid (MG) procedure for turbulent flows [9] and with local grid refinements [9,10], are used to simulate the indoor airflow. The MG method is an iterative procedure which ideally has a grid–independent convergence rate. Local grid refinements make it possible to resolve large gradients in the flow field without influencing the convergence rate of the MG scheme.

The conventional step–down method is a time–dependent solution of the advection–diffusion equation for a passive contaminant. Standard single–grid methods use constant or variable time steps, but all the computations are done on one fine spatial grid. For accuracy, it is unnecessary to use such a fine grid globally. Furthermore, the convergence of standard iterative methods is slower on fine grids than on coarse ones. The accurate solution of time–dependent flow problems with such methods is very expensive [11]. In this article, the multigrid method is used to speed up the prediction of the concentration as functions of space and time in ventilated rooms.

In the following sections, the local age and air change efficiency are discussed. The multigrid with a local grid–refined simulation of turbulent indoor airflow is described. Three new procedures are introduced: the transient MG method, the steady state MG method and the particle marker method. An example is used to compare and evaluate these methods.

LOCAL MEAN AGE AND AIR CHANGE EFFICIENCY

The air change efficiency, ε_a, is a measure of how effectively the air in a room is replaced by fresh air from the ventilation system. A value of 0.5 (50%) indicates a fully mixed ventilation, and a value of 1.0 (100%) represents a plug flow (or a unidirectional flow). The local air change index, ε_p, shows how quickly the air at a point P is replaced. ε_a and ε_p are defined as:

$$\epsilon_a = 100\frac{\tau_n}{\tau_r} = 100\frac{\tau_n}{2 < \tau >} \quad (\%) \tag{1}$$

$$\epsilon_p = 100\frac{\tau_n}{\tau_p} \quad (\%) \tag{2}$$

The local mean age of air is defined as the average time for air to travel from the inlet to any point P in the room:

$$\tau_P = \frac{\int_0^\infty t \cdot A_P(t)dt}{\int_0^\infty A_P(t)dt} \tag{3}$$

The mean age of the air at point P can be found from the centroid of the frequency distribution curve. The mean age of the room air is defined as the average of the local mean ages for all points in a room [12]:

$$<\tau> = \frac{1}{V}\int \tau_P dv \tag{4}$$

There are three main methods for finding the local and room mean ages of air: the pulse method, the tracer step–up method and the tracer decay method. Various equations for the local mean age and room mean age have been derived [12].

With a step–down method, the local mean age is found from:

$$\tau_P = \int_0^\infty \frac{c_P(t)}{c(0)} dt \tag{5}$$

The mean age of the room air, $<\bar{\tau}>$, can be calculated either from the average room concentration, $<c(t)>$, or from the exhaust concentration, $c_e(t)$:

$$<\tau> = \int_0^\infty \frac{<c(t)>}{c(0)} dt \tag{6}$$

$$<\tau> = \frac{\int_0^\infty t c_e(t) dt}{\int_0^\infty c_e(t) dt} \tag{7}$$

The above definitions illustrate the following:

1) The local mean age of air at a point P depends on the concentration changes at the point.

2) The average age of room air can be found from the local mean age field, from the average concentration changes in the room, and from the exhaust–inlet concentration changes. Only the exhaust–inlet concentrations can easily be measured. The local and room mean ages, $\bar{\tau}_P$ and $<\tau>$, can be more easily calculated than measured.

3) Tracer decay methods can be visualized as starting from a uniform concentration of passive contaminants at time $t = 0$ or a uniform distribution of particles in various computational cells. All particles start to move at time $t = 0$. The number of particles passing through the exhaust outlet is a measure of the concentration at the outlet. So particle numbers can be used to find the air change efficiency.

4) The local mean age and the mean age of room air are quantities that involve concentrations integrated from time $t = 0$ to $t = \infty$. With no contaminant generation, the concentration can be found from:

$$\frac{\partial c}{\partial t} + u\frac{\partial c}{\partial x} + v\frac{\partial c}{\partial y} + w\frac{\partial c}{\partial z} = \frac{\partial}{\partial x}\left[\frac{v_{eff}}{\sigma_c}\left(\frac{\partial c}{\partial x}\right)\right] + \frac{\partial}{\partial y}\left[\frac{v_{eff}}{\sigma_c}\left(\frac{\partial c}{\partial y}\right)\right] + \frac{\partial}{\partial z}\left[\frac{v_{eff}}{\sigma_c}\left(\frac{\partial c}{\partial z}\right)\right] \tag{8}$$

For equation (8), the boundary condition at the walls is $dc/dn = 0$, at the inlet $c = 0$, and at the outlet $dc/dy = 0$. The initial condition is $c(x,y,z) = c_0$, which is a homogeneous concentration of contaminant.

According to Sandberg [13,14], an equation for finding the local mean age can be obtained either by integrating equation (8) from $t = 0$ to $t = \infty$ (for the step–up and decay methods), or by multiplying equation (8) by t and then integrating from $t = 0$ to $t = \infty$ (pulse method):

$$u\frac{\partial\bar{\tau}}{\partial x}+v\frac{\partial\bar{\tau}}{\partial y}+w\frac{\partial\bar{\tau}}{\partial z} = \frac{\partial}{\partial x}\left[\frac{\nu_{eff}}{\sigma_\tau}\left(\frac{\partial\bar{\tau}}{\partial x}\right)\right]+\frac{\partial}{\partial y}\left[\frac{\nu_{eff}}{\sigma_\tau}\left(\frac{\partial\bar{\tau}}{\partial y}\right)\right]+\frac{\partial}{\partial z}\left[\frac{\nu_{eff}}{\sigma_\tau}\left(\frac{\partial\bar{\tau}}{\partial z}\right)\right]+1 \tag{9}$$

The boundary conditions are obtained as follows: at the inlet, it is assumed that there is no diffusion against the convective flow and $\tau_{in} = 0$; at the outlet, $d\bar{\tau}/dy = 0$ because $dc/dy = 0$. The boundary conditions at walls are obtained from $dc/dn = 0$:

$$\frac{\partial\int_0^\infty \frac{c}{c_0}dt}{\partial n} = 0 \qquad or \qquad \frac{\partial\bar{\tau}}{\partial n} = 0 \tag{10}$$

Equation (10) provides a steady–state numerical method for determining the local mean age, the room mean age, and the air change efficiency.

MULTIGRID SOLUTION FOR TURBULENT INDOOR AIRFLOW

To find the local mean age or air–change efficiency, the indoor flow field must be determined. It can be obtained both experimentally and numerically. Here, a multigrid prediction of the turbulent airflow field is described.

Governing Equations

The indoor airflow code VentAirII [15,16] solves the unsteady, Reynolds–averaged, Navier–Stokes equations, along with the k–ϵ model for closure. The equations can be written in the following conservation forms:

$$\frac{\partial\varrho u_i}{\partial x_i} = 0 \tag{11}$$

$$\frac{\partial\varrho u_i}{\partial t}+\frac{\partial\varrho u_i u_j}{\partial x_j} = -\frac{\partial p}{\partial x_j}+\frac{\partial}{\partial x_j}\left[\mu_{eff}\left(\frac{\partial u_i}{\partial x_j}+\frac{\partial u_j}{\partial x_i}\right)\right]-\varrho g_i \tag{12}$$

$$\frac{\partial\varrho k}{\partial t}+\frac{\partial\varrho k u_j}{\partial x_j} = \frac{\partial}{\partial x_i}\left[\frac{\mu_{eff}}{\sigma_k}\left(\frac{\partial k}{\partial x_i}\right)\right]+P+G-\varrho\epsilon \tag{13}$$

$$\frac{\partial\varrho\epsilon}{\partial t}+\frac{\partial\varrho\epsilon u_j}{\partial x_j} = \frac{\partial}{\partial x_i}\left[\frac{\mu_{eff}}{\sigma_\epsilon}\left(\frac{\partial\epsilon}{\partial x_i}\right)\right]+C_{1\epsilon}\frac{\epsilon}{k}(P+G)-C_{2\epsilon}\frac{\varrho\epsilon^2}{k} \tag{14}$$

$$\frac{\partial\varrho\theta}{\partial t}+\frac{\partial\varrho\theta u_j}{\partial x_j} = \frac{\partial}{\partial x_i}\left[\frac{\mu_{eff}}{\sigma_\theta}\left(\frac{\partial\theta}{\partial x_i}\right)\right]+S_\theta \tag{15}$$

where

$$\mu_{eff} = \mu+f_\mu C_\mu\varrho\frac{k^2}{\epsilon} = \mu+\mu_t \qquad P = \mu_t\left(\frac{\partial u_i}{\partial x_j}+\frac{\partial u_j}{\partial x_i}\right)\frac{\partial u_i}{\partial x_j} \qquad G = \beta g_i\frac{\mu_t}{\sigma_\theta}\frac{\partial\theta}{\partial x_i} \qquad S_\theta = \frac{Q}{C_p}$$

$C_{1\epsilon}=1.44 \qquad C_{2\epsilon}=1.92 \qquad \sigma_k=1.0 \qquad \sigma_\epsilon=1.3 \qquad \sigma_\mu=0.09 \qquad \sigma\theta=0.9$

In general $\rho = \rho(\theta)$. When the Boussinesq approximation is used, $\rho = \rho_{ref}$, where ρ_{ref} is the reference density. Then the buoyancy term in the momentum equation is replaced by $(\rho - \rho_{ref})g_i$.

All the variables are given for the supply inlets. The k and ε values are determined either by measurement or from an empirical formula. A zero–gradient condition applies to the exhaust outlets. At planes of symmetry, the normal gradient is zero for all quantities, and the normal velocity components and scalar fluxes are zero. At a wall boundary, Dirichlet boundary conditions are used, which are based on the wall functions.

Solution Procedure

In the VentAirII code [16], the physical domain is described by a global uniform rectangular mesh. The diffusive terms are approximated by the central difference scheme. The convective terms are approximated by the hybrid, central/upwind, difference scheme. The multi–grid (MG) procedure by Bai and Fuchs [9] is used. A four–level, V–cycle, multigrid, nodal configuration is shown in Fig. 1. The main ingredients of the MG method are the smoothing procedure, and the restriction and the prolongation operators. The restriction is achieved by volume averaging, and the prolongation by trilinear interpolation [17]. The Distributive–Gauss–Seidel (DGS) method is used to decouple the discrete continuity and momentum equations. The Symmetric Successive Point Relaxation (SSPR) method has been used as a smoother.

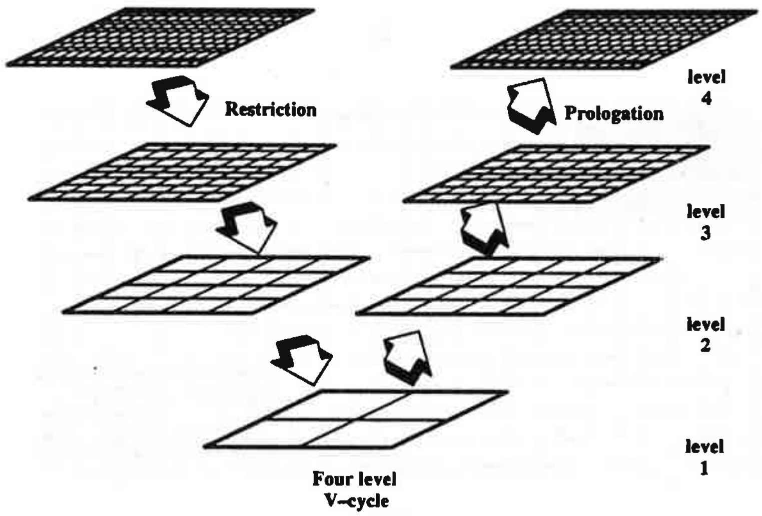

Fig. 1. A four–level, V–cycle, multigrid, nodal configuration.

The larger–gradient region can be resolved by other grids, such as uniform fine grids and non–uniform grids (Fig. 2). It is impractical to use uniformly fine grids, because of computer memory limitations and high computational costs. Both uniformly fine grids and non–uniform grids introduce fine grids at parts of the domain where they are not needed. In addition, for non–uniform grids, the details of the solution when the grid is generated must be known in advance, and additional storage (e.g. the locations of nodes) is needed. The MG scheme can be extended to include the local grid refinement. With this technique, developed by Fuchs [10], new sub–grids are introduced where the estimated truncation error is too large. The new local grids form new higher levels in the hierarchy of grids.

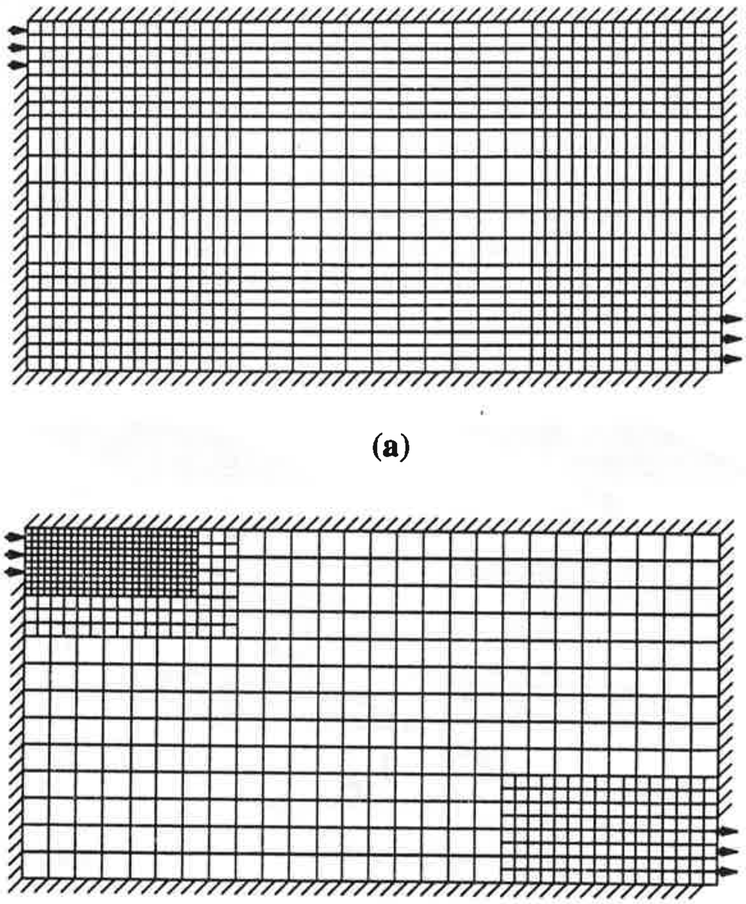

(a)

(b)

Fig. 2. (a) nonuniform grid; (b) local refined grid.

The solution given here is obtained from a four– to six–order–of–magnitude reduction in the L2–norm of the residual, defined in [16], from its maximum value.

FAST PROCEDURE FOR PREDICTING AGE AND AIR CHANGE EFFICIENCY

Transient Method

The flow field obtained numerically or experimentally can be used to calculate the local mean age and air change efficiency in various ways. The same procedure as the tracer gas experiment can be chosen, i.e. introduce passive contaminants and use a step–up, step–down or pulse method. Only step–down will be discussed here, but the technique is valid for other methods.

Equation (8) which will be solved is linear, since the contaminant is dynamically passive. This means that the velocity field and the diffusion coefficient field for the concentration equation are fixed. The decay of concentration is recorded at the points where the local age is to be found.

The concentration equation is approximated by using the central difference scheme, except in the convective term of equation (8) where the hybrid difference scheme is used. The time term is approximated by a Crank–Nicolson–like scheme:

$$\frac{c^{n+1} - c^{n}}{\Delta t} + \frac{1}{2} CD^{n} + \frac{1}{2} CD^{n+1} = 0 \tag{16}$$

where CD refers to the convection–diffusion terms using the above mentioned difference schemes. In each time step, the spatial problem is solved by an inner MG solver, as before.

Steady–State Method

There is no experimental method that corresponds to this numerical method. The method solves the steady–state equation of the local mean age. In theory, this method is superior to the transient method, since a time accurate solution of a time–dependent equation generally takes longer. The same difference schemes as before are used, except no time term is involved. The discrete equation is solved by the pseudo–time marching, steady–MG method [9].

Particle–Marker Method

This is similar to the transient method, but passive particles are used. Homogeneous particles start moving in the computational domain, e.g. one particle in each cell centre. The velocity of a particle at a point can be obtained as:

$$u_P = u_i \equiv \overline{u}_i + u_i' \tag{17}$$

Here the directions of u_i', v_i' and w_i' can be sampled by a random number generator. The magnitudes of u', v' and w' are assumed to be isotropic and can be obtained as:

$$\sqrt{\overline{u'^2}} = \sqrt{\overline{v'^2}} = \sqrt{\overline{w'^2}} = \sqrt{\frac{2k}{3}} \tag{18}$$

The position of the particle can be calculated by a trajectory equation:

$$\frac{dx_i}{dt} = u_P \qquad \frac{dy_i}{dt} = v_P \qquad \frac{dz_i}{dt} = w_P \tag{19}$$

$$x = x_0 + \Delta t u_P \qquad y = y_0 + \Delta t v_P \qquad z = z_0 + \Delta t w_p \tag{20}$$

where $\Delta t \leq \min(\Delta x/u_p, \Delta y/v_p, \Delta z/w_p)$, and Δx, Δy, Δz are the cell sizes.

Two situations can occur at the room boundaries: if a particle reaches the outlet, it is recorded; if it reaches the walls or the inlet, it returns. Here no back diffusion at inlet is assumed.

In practice, the fluctuating velocity, u_i', can probably be neglected. Considering convection alone gives quite reasonable results from an engineering point of view. If only the air change efficiency is needed, the particle–marker method is an economical choice.

EXAMPLE

To evaluate these numerical methods, the calculations are performed for an isothermal flow in a ventilated room of 5x5x4m^3 (Fig. 3). The supply air terminal is mounted centrally in a side wall with a diffuser (*jet killer*) to disperse the incoming air radially. The exhaust air terminal is placed on the opposite wall. This system has been tested and the experimental results for air change efficiency are available [18].

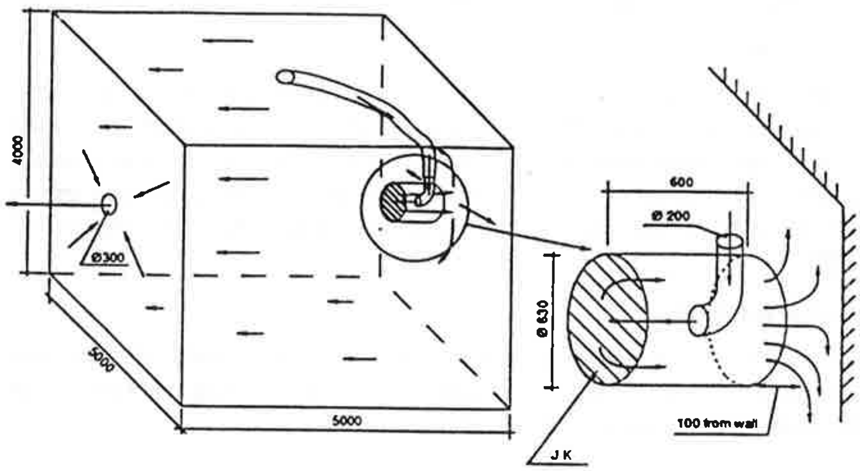

Fig. 3. The ventilated room (from [18])

Local Grid Refinement

Local grid refinement is used to refine the details of both geometry and physics at the inlet. The calculations have been performed for various geometries to investigate the effect of the jet killer on the flow field. Fig. 4–5 show that the velocity profiles at a vertical mid–plane. The air spreads out in a layer over the inlet wall and circulations are formed at the corners. The results agree well with the primary smoke test [19]. The grids used are the finest global mesh of 22*22*20 points and local refined mesh of 22*26*32 points. The VentAirII code shows a much faster convergence than corresponding single–grid methods for this isothermal problem.

Air Change Efficiency

The room in Fig. 3 is described with a global mesh of 50*50*50 points. The concentrations and particle number changes at the exhaust are compared in Fig. 6–7 for a specific flow rate of 1 and in Figs. 8–9 for a specific flow rate of 4. The measured and calculated air change efficiencies are shown in Table 1.

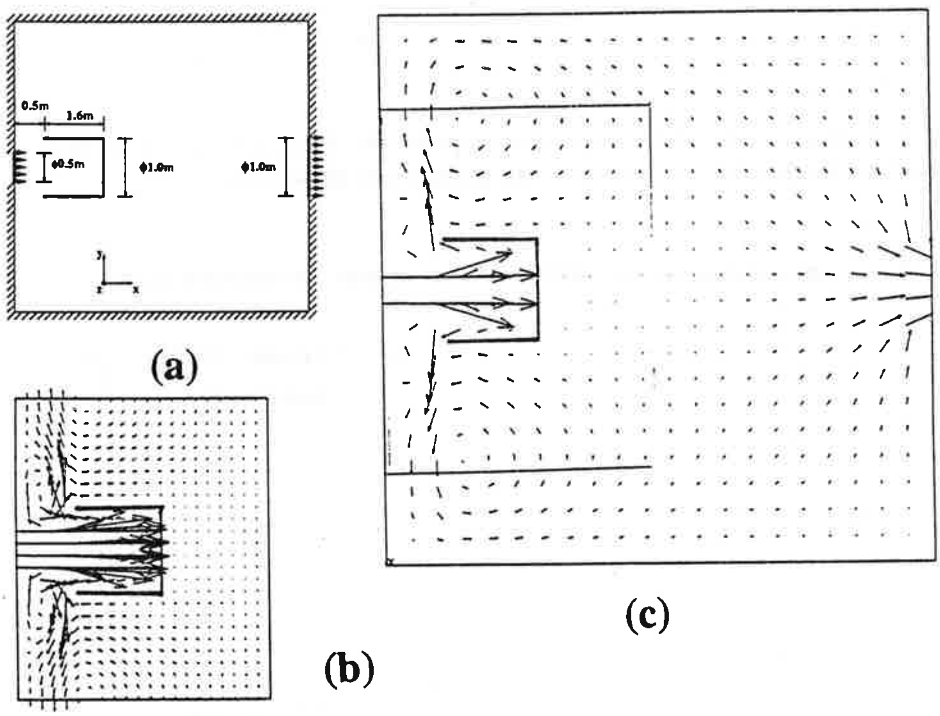

Fig. 4. Simulated flow fields for jet killer geometry No. 1. (a) geometry at vertical mid–plane; (b) flow with local refined grids; (c) flow with global grids.

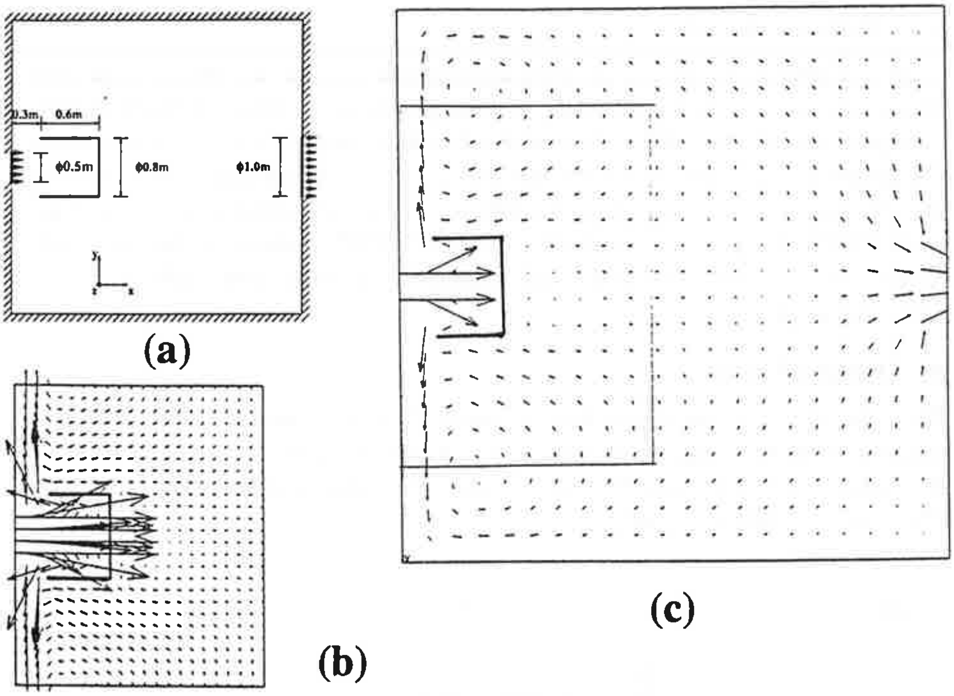

Fig. 5. Simulated flow fields for jet killer geometry No. 2. (a) geometry at vertical mid–plane; (b) flow with local refined grids; (c) flow with global grids.

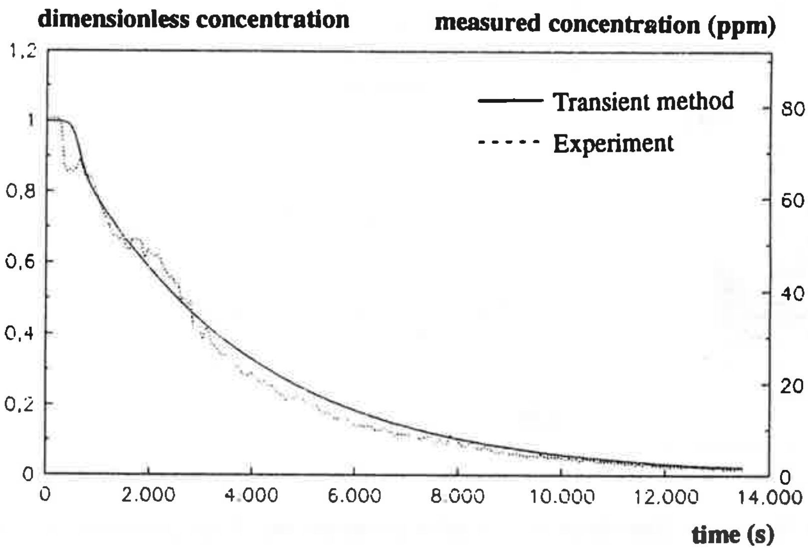

Fig. 6. Measured and calculated concentration changes at the exhaust outlet with a specific flow rate of 1.

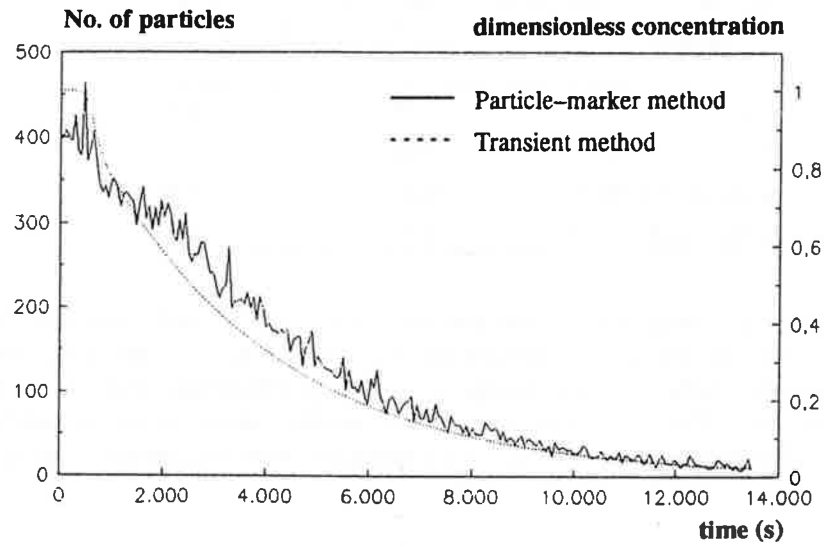

Fig. 7. Calculated concentration changes at the exhaust outlet with a specific flow rate of 1.

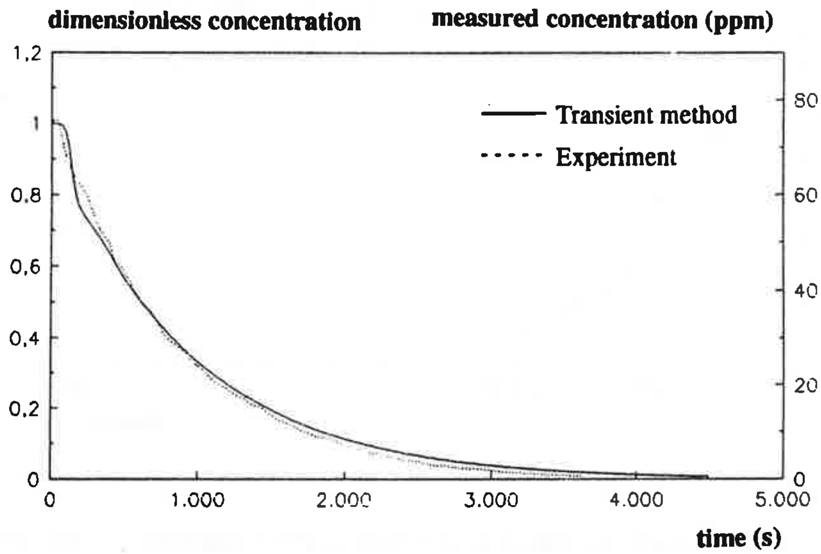

Fig. 8. Measured and calculated concentration changes at the exhaust outlet with a specific flow rate of 4.

Table 1. Measured and calculated air change efficiency.

Method	Specific Flow Rate	
	1	4
Measurement	0.59	0.58
Transient method	0.57	0.53
Steady–state method	0.57	0.53
Particle–marker method	0.58	0.55

The transient and steady–state methods give identical results. The steady–state method is generally faster than the transient method (in the example, about five times faster). The particle–marker method has the advantage of being easily implemented, and is almost as fast as the steady–state method when the number of particles generated equals the number of grids. The number of particles generated determines both computational cost and accuracy.

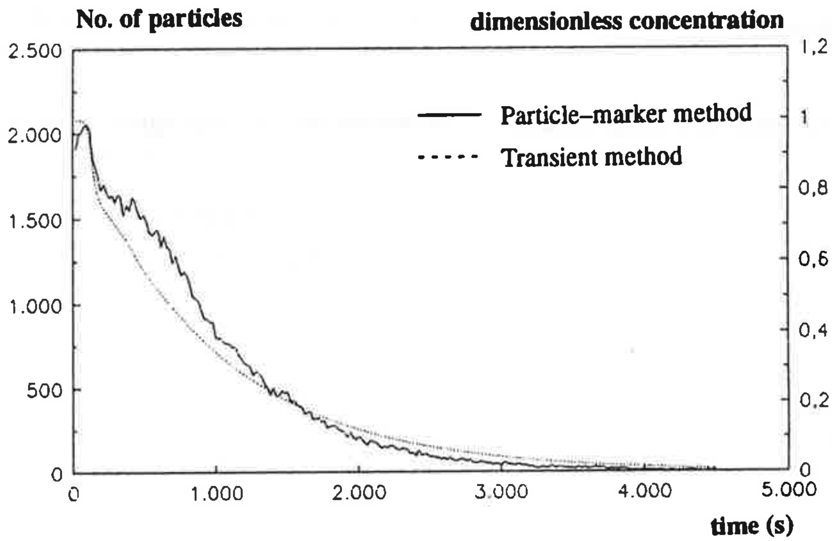

Fig. 9. Calculated concentration changes at the exhaust outlet with a specific flow rate of 4.

CONCLUSIONS

Three numerical methods for predicting air age and air change efficiency in ventilated rooms are developed and evaluated. These include a transient method in which a time-dependent concentration equation is solved, a steady-state method in which a steady state-equation of air age is solved, and a particle-marker method, in which no partial differential equation is involved. In the first two methods, a multigrid method is used. An efficient multigrid prediction of turbulent indoor airflow is also suggested, which provides the air velocity and turbulent effective viscosity fields to predict air age. Numerical evaluations for a test room show that the first two methods are efficient and reliable for predicting the local mean age of the indoor air, and the third method is efficient and reliable for predicting air change efficiency. The methods have not been evaluated in non-isothermal ventilated room and need to be investigated.

ACKNOWLEDGEMENT

The authors are grateful to Mr. Tyrrell Burt for checking the language. The work was financially supported by the Swedish Council for Building Research (BFR).

LIST OF SYMBOLS

$A_P(t)$	frequency function for air arriving at point P
c	concentration
$c_P(t)$	concentration of tracer at point P after time t
$c(0)$	initial concentration in the room
C_p	heat capacity of constant pressure
$C_{1\varepsilon}$, $C_{2\varepsilon}$	constants in turbulence model
g_i	gravitational acceleration in direction x_i
k	turbulent kinetic energy
n	axis normal to surface
p	pressure
Q	internal heat generation rate
t	time
u	velocity in x-direction
$\overline{u}_i$	mean velocity of air in ith cell
u_i'	fluctuating velocity in ith cell
u_P	particle velocity at point P
v	velocity in y-direction
w	velocity in z-direction
V	room volume
β	expansion coefficient
ε	dissipation rate of turbulence
θ	temperature
μ_{eff}	sum of the kinematic laminar viscosity μ and kinematic turbulent viscosity μ_t
ρ	density

σ_c turbulent Prandtl number for concentration
σ_k turbulent Prandtl number for turbulent kinetic energy
σ_ε turbulent Prandtl number for dissipation of turbulent kinetic energy
σ_θ turbulent Prandtl number for dissipation of turbulent kinetic energy
σ_τ turbulent Prandtl number for age of air
$\bar{\tau}_P$ local mean age of air at point P
τ_n nominal time constant
$\bar{\tau}_r$ air change time
$<\bar{\tau}>$ mean age of the room air

LITERATURE

[1] Sandberg, M. "**Ventilation efficiency as a guide to design**". ASHRAE Transactions, Vol.89, part 2B, (1983).

[2] Liddament, M.W. "**A review and bibliography of ventilation effectiveness – definitions, measurement, design and calculation**". Technical Note AIVC 21, July, (1987).

[3] Skaret, E., Mathisen, H.M. "**Ventilation efficiency–A guide to efficient ventilation**". ASHRAE Transactions, Vol.89, part 2B, (1983).

[4] Sandberg, M. "**The ventilation effectiveness in office buildings and its effects on indoor air quality**". ASHRAE Symposium on Indoor Air Quality and Energy Consumption. Montreal, Canada, September 30, (1991).

[5] Sandberg, M. "**Contaminant exposures, age distribution of air and contaminants in a ventilated room**". ,TM279 (in Swedish), Department of Heating and Ventilation, Royal Institute of Technology, Stockholm, Sweden, (1984).

[6] Roulet, C–A., Compagnon, R., Jakob, M. "**A simple method using tracer gas to identify the main air and contaminant paths within a room**". Proceedings of 11th AIVC Conference, pp. 265–277, Belgirate, Italy, 18–21, September (1990).

[7] Davidson, L., Olsson, E. "**Calculation of age and local purging flow rate in rooms**". Building and Environment, Vol. 22, pp.111–127, (1987).

[8] Fontaine, J.R., Gardin, P., Soumoy, V., Aubertin, G. "**Criteria for the evaluation of general ventilation systems: Numerical and physical simulations**". Proceedings of Ventilation'88. 2nd International Symposium on Ventilation for Contaminant Control, Londres, 20–23, September, (1988).

[9] Bai, X.S., Fuchs, L. "**A fast multi–grid method for 3–D turbulent incompressible flows**". 7th International Conference on Numerical Methods in Laminar and Turbulent Flow, Stanford, California, 15th–19th, July, (1991).

[10] Fuchs, L. "**A local mesh–refinement technique for incompressible flows**". Computers & Fluids, Vol.14, No.1, pp.69–81, (1986).

[11] Karlsson, A., Fuchs, L. "**Fast and accurate solution of time–dependent incompressible flow**". Numerical Methods in Laminar and Turbulent Flow–III. Eds. C. Taylor, J.A. Johnson and W.R. Smith. Pineridge Press, pp.606–616, (1983)

[12] Sutcliffe, H. "**A guide to air change efficiency**". AIVC, (1990).

[13] Sandberg, M. "**What is ventilation efficiency**". Building and Environment, Vol.16, No.2, pp.123–135, (1981).

[14] Sandberg, M., Sjöberg, M. "**The use of moments for assessing air quality in ventilated rooms**". Building and Environment, Vol.18, No.4, pp.181–197, (1983).

[15] Li, Y, Fuchs, L. "**Accurate numerical simulation of air flows in ventilated multi–rooms**". Building Simulation'91 Conference, Nice, France, August 20–22, (1991).

[16] Li., Y., Fuchs, L., Holmberg, S. "**An evaluation of a computer code for predicting indoor airflow and heat transfer**". 12th AIVC Conference, Ottawa, Canada, 24–27 September, (1991).

[17] Fuchs, L., Zhao, H.S. "**Solution of three–dimensional viscous incompressible flows by a multi–grid method**". International Journal for Numerical Methods in Fluids. Vol.4, 539–555, (1984).

[18] Tang, Y.–Q., Holmberg, S. "**An experimental investigation of a horizontal displacement ventilation system**", Research report 1992:2, National Institute of Occupational Health, Stockholm, (1992).

[19] Holmberg, S., Li, Y., Fuchs, L. "**Ventilation by vertical and horizontal displacement – a numerical comparison of air change efficiency and thermal comfort parameters**". Proceedings of Ventilation'91, Cincinnati, Ohio, 16–19, September, (1991).